

Multiphonon Processes in Atom-Surface Scattering

V. Celli, D. Himes, and P. Tran

University of Virginia, Charlottesville, Virginia 22901

J. P. Toennies, Ch. Wöll, and G. Zhang

Max-Planck-Institut für Strömungsforschung, D-3400 Göttingen, Germany

(Received 28 June 1990; revised manuscript received 20 May 1991)

Helium-atom time-of-flight spectra taken at 69-meV incident energy in scattering from Pt(111) show energy-loss peaks that cannot be assigned to one-phonon transitions, but are qualitatively explained by simple formulas for the multiphonon processes in the classical limit. This assignment is supported by trajectory-approximation calculations that correctly reproduce the experimentally determined density of states of Pt(111).

PACS numbers: 63.20.-e, 68.35.-p, 79.20.Rf, 82.65.My

The elementary collision processes leading to the accommodation and sticking¹ of closed-shell atoms on metal surfaces are still not well understood. It is generally accepted that electron-hole pair excitation is very improbable and that phonon interactions are the dominant mechanism for incident energies up to at least 100 meV.² Most previous surface scattering experiments can be classified into two categories: (1) single-phonon inelastic scattering involving mostly He atoms with the aim of measuring surface-phonon dispersion curves,³ and (2) classical-limit inelastic scattering involving heavy atoms or molecules (e.g., Ar, NO) where a significant fraction of the initial kinetic energy is lost.⁴ The latter experiments can be largely explained using simple dynamical models such as the hard-cube model¹ or classical trajectory calculations.⁵ To gain more insight into the details of multiphonon interactions we have carried out helium-atom-scattering (HAS) experiments under conditions intermediate between these two extremes.

For measuring the surface-phonon dispersion curves of metals, typically He atoms with incident energy $E_i = 10\text{--}40$ meV are used, and the scattered atoms are analyzed by their time of flight (TOF). Under these conditions, the single-phonon processes dominate or at least can be clearly resolved above the multiphonon background. It is usually assumed that this background is structureless in the region where one-phonon transitions occur. Thus, for a given set of incident and final scattering angles, a sharp peak at energy transfer ΔE and momentum transfer ΔK in the surface plane can be assigned to the creation ($\Delta E < 0$) or annihilation of a single surface phonon. Sharp multiphonon energy-loss features, in the form of overtones of a nearly dispersionless Einstein oscillator, have been observed only in the scattering from rare-gas overlayers⁶ and molecular adsorbates.⁷

In this Letter we present new He TOF spectra for a clean Pt(111) surface, taken at $E_i = 69$ meV, which show both one-phonon peaks and characteristic multiphonon

peaks not previously recognized as such. These multiphonon peaks trace out an apparent dispersion curve which could be interpreted as a new kind of excitation. We show, however, that they can be explained qualitatively by an adaptation of the Brako-Newns⁸ semiclassical formula for energy and momentum exchange in the trajectory approximation (TA). We also present a full quantum-mechanical TA calculation that accounts for both one-phonon and multiphonon processes.

The HAS-TOF apparatus has been described in detail in Ref. 9. By expanding the He from high pressure of about 100 bars through a small nozzle of 10 μm diameter, at a source temperature of 320 K, we obtain a He beam with a velocity spread of typically 1.2%–1.5%. The angle θ_{sd} between the incident and outgoing beams was fixed at 90° and different momentum transfers were obtained by rotating the crystal. The Pt(111) single crystal was prepared *in situ* at about 5×10^{-11} mbar until a clean single-crystal surface as characterized by LEED and a cylindrical-mirror Auger analyzer was obtained. Pt(111) was chosen for this exploratory study because the one-phonon scattering has recently been extensively studied both theoretically and experimentally.⁹ All data presented here were taken along the (110) azimuth at a surface temperature of $T = 160$ K.

Four representative TOF spectra, transformed to an energy-transfer abscissa, are shown by the histograms in Fig. 1. All spectra show a sharp elastic peak at $\Delta E = 0$ which is caused by scattering from surface defects.¹⁰ At $\theta_i = 40.2^\circ$, there is an inelastic peak, marked by a cross, that is attributed to the creation of a single surface phonon. With decreasing incident angle, however, the inelastic peak, marked by a circle, shifts to larger energy transfers which extend to well beyond the maximum possible for single-phonon excitations. The explanation of these anomalous peaks is our main concern here.

Each TOF spectrum represents the scattered intensity along a "scan curve" through the $(\Delta E, \Delta K)$ plane. For the fixed-angle $\theta_{sd} = 90^\circ$ apparatus used here, the scan

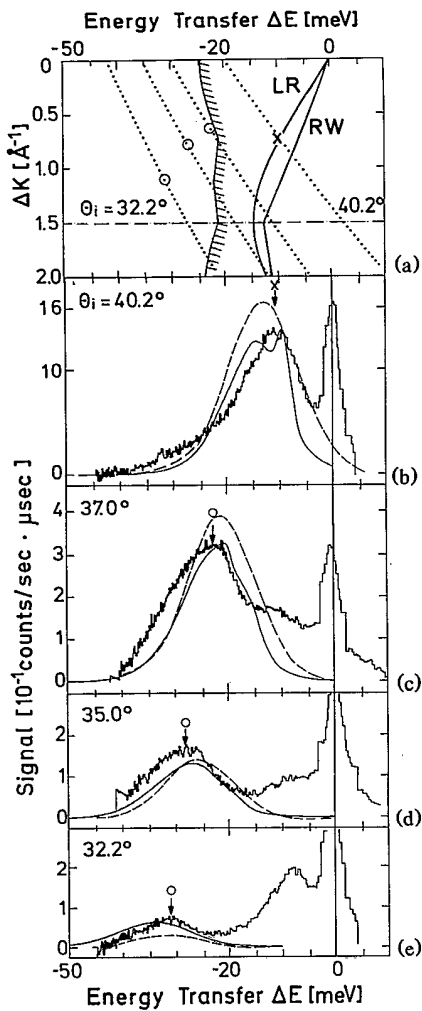


FIG. 1. (a) Scan curves and phonon spectrum; (b)–(e) density of scattered He atoms as a function of energy transfer ΔE for Pt(111) in the $\langle 110 \rangle$ azimuth. Incident energy $E_i = 69$ meV; surface temperature $T = 160$ K. Each scan curve, shown by a dotted line in (a), corresponds to a scattered density distribution in (b)–(e); a multiphonon maximum is marked by a circle, a one-phonon maximum by a cross. In (a) we also show the Rayleigh phonon RW and the longitudinal surface resonance LR (continuous lines), and the maximum one-phonon energy (line with shading). In (b)–(e) we show the experimental data (histograms), the Brako-News approximation (dashed lines), and the TA calculation (continuous lines).

curve is given by

$$\Delta E = E_i \left(\frac{(\sin\theta_i + \Delta E/k_i)^2}{\cos^2\theta_i} - 1 \right). \quad (1)$$

The scan curves for the four TOF spectra in Fig. 1 are shown in Fig. 1(a). They facilitate the assignment of the observed energy-loss features in relation to the one-phonon spectrum, which is also shown in outline.

TOF spectra have been measured for θ_i between 28° and 43° at intervals of 1° or less. The results are summarized in Fig. 2(a) by contour lines of equal scattered

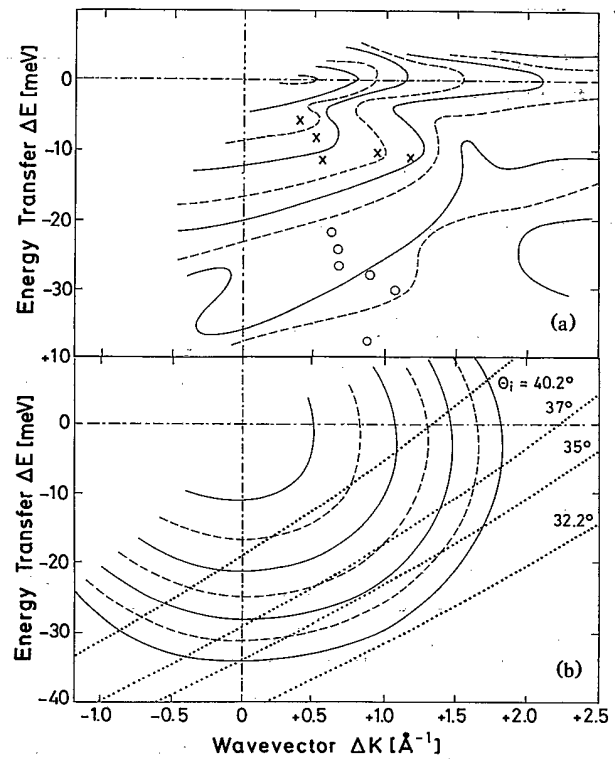


FIG. 2. Contours of equal scattered He density I in the energy-transfer-momentum-transfer plane, for the same system as in Fig. 1. (a) Experiment; (b) theory in the Brako-News approximation. $I(\Delta E, \Delta K)$ changes by a factor of 2 from one contour to the next. The dotted lines in (b) show the same scan curves as in Fig. 1(a). Circles and crosses mark maxima, as explained in the text.

particle density. Further, circles mark the location of anomalous maxima, such as those in Figs. 1(c)–1(e), and crosses mark the location of other inelastic maxima, such as that in Fig. 1(b). Two apparent dispersion curves are suggested by these data. The crosses extend from the origin out to the zone boundary at 1.51 \AA^{-1} with a maximum ΔE of 12 meV, in agreement with the known surface-phonon branches.⁹ The circles, on the other hand, extend to much larger energy transfers, into the region with $\Delta E > 25$ meV where single-phonon excitations are no longer possible. We show below that these anomalous maxima arise from multiphonon processes. It is interesting to point out that a similar anomaly was observed by Feuerbacher and Willis for Ne/Ni(111) scattering but was incorrectly attributed to a cutoff effect.¹¹

As discussed by Weare,¹² one can estimate that multiphonon processes are negligible when $W \ll 1$, where W is the Debye-Waller exponent for an impulsive He-surface collision:

$$W = [24\mu T(D + E_i \cos^2\theta_i)]/k_B T_D^2. \quad (2)$$

Here μ is the ratio of the He mass to that of a surface atom (assuming a monatomic surface), D is an effective

surface well depth, and T_D is the effective surface Debye temperature. For He/Pt(111), $\mu = 0.0205$, $T_D = 231$ K, and $D = 12$ meV.¹³ Thus our experiments are in a range ($0.9 < W < 1.05$ for the curves of Fig. 1) where one-phonon peaks are still clearly visible, but multiphonon processes have greater integrated intensity. In the forced-oscillator model, the n -phonon intensity is $e^{-2W}(2W)^n/n!$.¹⁴ For $W=1$, this Poisson formula gives 0.135 for the elastic, 0.271 for the one-phonon, and 0.594 for all the rest of the intensity.

Thus we need to go beyond the one-phonon theory in computing the probability of transferring energy ΔE and lateral momentum ΔK to the He atom during the collision. In the classical TA this probability, which we denote by $N(\Delta E, \Delta K)$, is a Gaussian centered at the average energy and momentum transfers, $\overline{\Delta E}$ and $\overline{\Delta K}$.¹⁵ To estimate $\overline{\Delta E}$, we use the Baule formula,¹ which is obtained by approximating the surface scattering with an atom-atom (He-Pt) collision that conserves momentum parallel to the surface:

$$\overline{\Delta E} = -\frac{4\mu}{(1+\mu)^2} [E_i \cos^2 \theta_i + D]. \quad (3)$$

We also take $\overline{\Delta K} = 0$, although this is strictly true only at normal incidence. We still need the width of the Gaussian, which we take from the work of Brako and Newns.⁸ Using the assumption that $T \gg T_D$ and that the process is dominated by low-frequency phonons belonging to a single surface-phonon branch with linear dispersion $\omega_Q = vQ$, these authors obtain

$$N(\Delta E, \Delta K) = N_0 \exp \left[-\frac{(\Delta E - \overline{\Delta E})^2 + 2\hbar^2 v^2 \Delta K^2}{4k_B T |\overline{\Delta E}|} \right], \quad (4)$$

with $N_0 = \hbar^2 v^2 / (\pi k_B T |\overline{\Delta E}|)^{3/2}$. We found that Eqs. (3) and (4) give a good explanation of the anomalous peaks, with only v as an adjustable parameter. We have taken $\hbar v = 12.5$ meV Å, which is the velocity of the longitudinal resonance (LR), shown in Fig. 1(a). This surface resonance is known to have a high spectral density⁹ and lies in the middle of the phonon spectrum.

The detected beam density at angle θ_f is $I = [2M(E_i + \Delta E)]^{1/2} \cos \theta_f N(\Delta E, \Delta K)$, with ΔE and ΔK related by Eq. (1). This quantity, with N given by Eq. (4), is plotted as a dashed line in Figs. 1(b)-1(e). Also, the contours of equal I in the $(\Delta E, \Delta K)$ plane are plotted in Fig. 2(b) for comparison with the experimental con-

tours of Fig. 2(a). For a given θ_i the contours of a product of Gaussian distributions along the ΔK and ΔE directions are, of course, ellipses. However, $\overline{\Delta E}$ changes with θ_i according to Eq. (3), and the contour lines shown in Fig. 2(b) are obtained by joining equal- I points on each scan curve. It can be seen from Fig. 2(b) that the observation of maxima in the energy-loss spectra which are shifted away from $\Delta K = 0$ is in fact due to a kinematic effect. The scan curves, shown by dotted lines for the representative spectra of Fig. 1, cross the equal- I contours at about 45° and thus produce broad maxima which lie along an apparent dispersion curve differing from the one-phonon dispersion curve.

We still must show that the simple Brako-Newns-Baule formula has a significant range of validity in the $(\Delta E, \Delta K)$ plane in our case, which is rather far from the classical limit.¹⁶ The Gaussian approximation, although good for large ΔE and ΔK and fair on the average, could smooth out some sharp structures. Also, the Brako-Newns estimate of the Gaussian widths is valid for $T/T_D > 1$, while in our case $T/T_D = 160/231$; finally, the Baule formula is only a rough estimate.

We have carried out a full TA calculation that is based on the published Pt(111) surface-phonon density of states and He-surface interaction and thus has, in principle, no adjustable parameters. We outline the method here, with emphasis on its new features.

We denote with \mathbf{u}_l the displacement of a surface atom from its equilibrium position \mathbf{R}_l . We expand \mathbf{u}_l in the operators $b_{\mathbf{Q}j}$ and $b_{\mathbf{Q}j}^\dagger$ that annihilate and create a phonon characterized by the lateral wave number \mathbf{Q} (in the x - y plane) and by the branch index j , and we denote the phonon frequencies by $\omega_{\mathbf{Q}j}$. A trajectory of the He atom is characterized by the impact parameter \mathbf{R} , which can be regarded as the starting (x, y) position on a reference plane far from the surface. As it moves along its trajectory, the He atom exerts a force $\mathbf{F}_l(\mathbf{R}, t)$ on the l th surface atom. The effective Hamiltonian for the collision can then be written as

$$H(\mathbf{R}, t) = \sum_{\mathbf{Q}j} \hbar \omega_{\mathbf{Q}j} b_{\mathbf{Q}j}^\dagger b_{\mathbf{Q}j} + \sum_l \mathbf{u}_l \cdot \mathbf{F}_l(\mathbf{R}, t). \quad (5)$$

The explicit form of the forcing functions $\mathbf{F}_l(\mathbf{R}, t)$ will be specified below. $H(\mathbf{R}, t)$ describes a set of forced harmonic oscillators and defines an exactly soluble problem. The resulting distribution $N(\Delta E, \Delta K)$ is simply the Fourier transform in \mathbf{R} and t of $\exp[\Gamma(\mathbf{R}, t) - 2W]$, where $\Gamma(\mathbf{R}, t)$ is linearly related to the correlation functions $\langle \mathbf{u}_l(t) \mathbf{u}_{l'}(t') \rangle$. Explicitly,

$$\Gamma(\mathbf{R}, t) = \frac{1}{2\hbar^2} \sum_{l'} \int d\tau d\tau' \mathbf{F}_l(0, -\tau) \cdot \langle \mathbf{u}_l(\tau) \mathbf{u}_{l'}(\tau') \rangle \cdot \mathbf{F}_{l'}(\mathbf{R}, t - \tau'). \quad (6)$$

W is, in principle, the exact Debye-Waller exponent and $2W = \Gamma(\mathbf{R} = 0, t = 0)$.

When $\exp[\Gamma(\mathbf{R}, t)]$ is expanded as $1 + \Gamma(\mathbf{R}, t) + \dots$, we see that the term linear in Γ gives the one-phonon processes. Thus we are able to fix $\Gamma(\mathbf{R}, t)$ by imposing that it must yield the same cross section for the one-phonon processes as the distorted-wave Born approximation. In this way we determine $\mathbf{F}_l(\mathbf{R}, t)$, or equivalently,

$$F(\mathbf{Q}, \omega) = e^{i\mathbf{Q} \cdot \mathbf{R}_l} \int \mathbf{F}_l(\mathbf{R}, t) e^{i(\omega t - \mathbf{Q} \cdot \mathbf{R})} dt d\mathbf{R},$$

which does not depend on l . In the case of the Pt(111) surface, where the static corrugation is negligible, the eigenfunctions of the static He-surface potential V are of the form $\chi(z)e^{i\mathbf{K}\cdot\mathbf{R}}$. For the transition from \mathbf{K}_i to $\mathbf{K}_i + \Delta\mathbf{K}$ and from E_i to $E_i + \Delta E$, we identify \mathbf{Q} with $\Delta\mathbf{K}$ and $\hbar\omega$ with ΔE . Then

$$F(\mathbf{Q}, \omega) = \int \chi_f^*(z) F(\mathbf{Q}, z) \chi_i(z) dz,$$

where

$$F(\mathbf{Q}, z) = e^{i\mathbf{Q}\cdot\mathbf{R}_i} \int \mathbf{V}_l V e^{-i\mathbf{Q}\cdot\mathbf{R}} d\mathbf{R}.$$

The dependence on ω comes from the fact that χ_f depends on the final perpendicular energy. When V is a sum of pairwise potentials, $F(\mathbf{Q}, z)$ is the Fourier transform of the pairwise force between the He atom and a surface atom.

In the application of this method reported here, we have used $F(\mathbf{Q}, \omega) = (\hat{z} + i\mathbf{Q}/\beta) F_z(Q)$, where

$$|F_z(Q)|^2 = (8m/\hbar^2)(E_i \cos^2\theta_i + D) \exp(-Q^2/Q_c^2),$$

with $\beta = 1.83 \text{ \AA}^{-1}$ and $Q_c = 0.57 \text{ \AA}^{-1}$. This model interaction, corresponding to hard-wall matrix elements for specular reflection modified by a Gaussian factor that accounts for softness, has proven successful in explaining the inelastic scattering from smooth (111) metal surfaces at lower incident energies.⁹ The results are given by the solid lines in Fig. 1. They have been normalized to the data at $\theta_i = 35.0^\circ$. In all four spectra of Fig. 1, the full TA calculation provides a better fit of the shape and of the relative intensities than the Brako-Newns-Baule formula.

The extra intensity seen in the data close to the incoherent elastic peak can be attributed mostly to incoherent inelastic scattering. The feature apparent at 8 meV in the spectrum of Fig. 1(e), and present in other spectra not shown, is consistent with a surface phonon having ΔK on the second Brillouin-zone boundary. Our present TA calculation does not extend this far in ΔK .

In conclusion, we have been able to explain new energy-loss features occurring at incident He energies only slightly greater than those optimum for single-phonon coupling: They are due to multiphonon processes. From an experimental point of view, our findings show how to identify and subtract the multiphonon "background," thus opening the way to a more accurate determination of the one-phonon intensities. From a general theoretical point of view, we are able to fully describe the abrupt transition from the extreme quantum limit, where the one-phonon processes dominate the TOF spectra, to the classical limit. We have identified a

characteristic and general signature of the energy-loss spectra that is present in this intermediate regime. Finally, we note that the new version of the TA described here makes it possible to investigate the technologically important processes of sticking and accommodation on clean surfaces with a theory based on a realistic description of the surface-projected phonon density of states.

We are indebted to G. Santoro for the programs to generate the Pt(111) phonon spectra, to V. Bortolani and J. R. Manson for helpful discussions, and to J. Black for a critical reading of the manuscript. This work was supported by the A. von Humboldt Foundation, by NATO Grant No. 33-0673/88, and by NSF Grant No. INT-8913115.

¹F. O. Goodman and H. Y. Wachman, *Dynamics of Gas-Surface Scattering* (Academic, New York, 1976).

²O. Gunnarson and K. Schönhammer, in *Many Body Phenomena at Surfaces*, edited by D. Langreth and H. Suhl (Academic, Orlando, 1984), p. 421.

³J. P. Toennies, in *Solvay Conference on Surface Science*, edited by F. W. de Wette (Springer, Berlin, 1988), p. 248.

⁴J. E. Hurst, L. Wharton, K. C. Janda, and D. J. Auerbach, *J. Chem. Phys.* **78**, 1559 (1983).

⁵D. C. Jacobs and R. N. Zare, *J. Chem. Phys.* **91**, 3196 (1989).

⁶K. D. Gibson, S. J. Sibener, B. M. Hall, D. L. Mills, and J. E. Black, *J. Chem. Phys.* **83**, 4256 (1985).

⁷A. M. Lahee, J. P. Toennies, and Ch. Wöll, *Surf. Sci.* **177**, 371 (1986).

⁸R. Brako and D. M. Newns, *Phys. Lett.* **48**, 1859 (1982); *Surf. Sci.* **117**, 42 (1982).

⁹V. Bortolani, A. Franchini, G. Santoro, J. P. Toennies, Ch. Wöll, and G. Zhang, *Phys. Rev. B* **40**, 3524 (1989).

¹⁰A. Lahee, J. R. Manson, J. P. Toennies, and Ch. Wöll, *Phys. Rev. Lett.* **57**, 471 (1986).

¹¹B. Feuerbacher and R. F. Willis, *Phys. Rev. Lett.* **47**, 526 (1981).

¹²J. H. Weare, *J. Chem. Phys.* **61**, 2900 (1974).

¹³V. Bortolani, V. Celli, A. Franchini, J. Idiodi, G. Santoro, K. Kern, B. Poelsema, and G. Comsa, *Surf. Sci.* **208**, 1 (1989).

¹⁴G. Armand and P. Zeppenfeld, *Phys. Rev. B* **40**, 5936 (1989).

¹⁵For a review of the TA, see V. Bortolani and A. C. Levi, *Riv. Nuovo Cimento* **9**, No. 11, 1 (1986). For a recent discussion, see K. Burke, J. H. Jensen, and W. Kohn, *Surf. Sci.* **241**, 211 (1991).

¹⁶The prediction that the widths increase at $T^{1/2}$ and the height decreases as $T^{-3/2}$ is only valid in the limit $W \gg 1$, when the elastic peak has vanished; for $W \approx 1$ the inelastic scattering is still growing at the expense of the elastic. See J. R. Manson (to be published).